Available online at www.sciencedirect.com
ScienceDirect
Nuclear Physics A 801 (2008) 101–113
NUCLEAR PHYSICS A
www.elsevier.com/locate/nuclphysa

Production of nuclei in neutron unbound states via primary fragmentation of ^{48}Ca

G. Christian [a,b], W.A. Peters [a,b,1], D. Absalon [c], D. Albertson [a,b], T. Baumann [a], D. Bazin [a], E. Breitbach [c], J. Brown [d], P.L. Cole [e], D. Denby [f], P.A. DeYoung [f], J.E. Finck [g], N. Frank [a,b,2], A. Fritsch [d], C. Hall [f], A.M. Hayes [a,b], J. Hinnefeld [h], C.R. Hoffman [i], R. Howes [c], B. Luther [e], E. Mosby [j], S. Mosby [j], D. Padilla [f], P.V. Pancella [k], G. Peaslee [f], W.F. Rogers [j], A. Schiller [l], M.J. Strongman [a,b], M. Thoennessen [a,b,*], L.O. Wagner [e]

[a] *National Superconducting Cyclotron Laboratory, Michigan State University, East Lansing, MI 48824, USA*
[b] *Department of Physics and Astronomy, Michigan State University, East Lansing, MI 48824, USA*
[c] *Department of Physics, Marquette University, Milwaukee, WI 53201, USA*
[d] *Department of Physics, Wabash College, Crawfordsville, IN 47933, USA*
[e] *Department of Physics, Concordia College, Moorhead, MN 56562, USA*
[f] *Department of Physics, Hope College, Holland, MI 49423, USA*
[g] *Department of Physics, Central Michigan University, Mt. Pleasant, MI 48859, USA*
[h] *Department of Physics and Astronomy, Indiana University at South Bend, South Bend, IN 46634, USA*
[i] *Department of Physics, Florida State University, Tallahassee, FL 32306, USA*
[j] *Department of Physics, Westmont College, Santa Barbara, CA 93108, USA*
[k] *Physics Department, Western Michigan University, Kalamazoo, MI 49007, USA*
[l] *Department of Physics and Astronomy, Ohio University, Athens, OH 45701, USA*

Received 28 November 2007; accepted 8 January 2008

Available online 16 January 2008

* Corresponding author at: National Superconducting Cyclotron Laboratory, Michigan State University, East Lansing, MI 48824, USA.
E-mail address: thoennessen@nscl.msu.edu (M. Thoennessen).
[1] Present address: Department of Physics & Astronomy, Rutgers, The State University of New Jersey, Piscataway, NJ 08854, USA.
[2] Present address: Physics Department, Illinois Wesleyan University, Bloomington, IL 61701, USA.

0375-9474/$ – see front matter
doi:10.1016/j.nuclphysa.2008.01.004

Abstract

The method of sequential neutron decay spectroscopy beginning with a primary beam of 60 MeV/nucleon ^{48}Ca was investigated as a potential tool to measure unbound resonances in neutron-rich nuclei. Neutrons were measured in coincidence with fragments, and unbound resonances were observed for ^{10}Li, ^{12,13}Be, and ^{23}O. The method is currently limited to resonances with small decay energies ($E_{\text{decay}} \lesssim 100$ keV) in lighter ($Z \leqslant 10$) nuclei, and the possibility of extending it to heavier, more neutron-rich nuclei will be discussed.

PACS: 21.10.Pc; 23.90.+w; 25.70.-z; 29.30.Hs

Keywords: NUCLEAR REACTION Be(^{48}Ca, X), $E = 60$ MeV/nucleon; measured fragment and neutron energies and yields. ^{10}Li, ^{12,13}Be, ^{23}O; observed unbound resonances

1. Introduction

The structure of nuclei close to the neutron dripline is difficult to study with γ-ray spectroscopy because these nuclei have few or no bound excited states. Thus other techniques have to be employed to observe these unbound excited states, whose decay is dominated by neutron emission. Single and multiple particle transfer reactions from stable beams have been used to populate and characterize unbound states in lighter ($Z \leqslant 4$) neutron-rich nuclei [1,2]. In order to populate heavier nuclei close to the dripline, radioactive beams are required. In addition to transfer reactions [3–6], β-delayed neutron spectroscopy [7–9] and invariant mass measurements following knockout reactions [6,10,11] have also utilized radioactive beams.

An alternative method to populate excited states of very neutron-rich nuclei with stable beams is sequential neutron decay spectroscopy (SNDS). In this method, the excited nuclei are produced in heavy-ion reactions and the decay fragments are measured in coincidence with the emitted neutrons in a collinear geometry. In the initial experiments the fragments and neutrons were detected at large angles relative to the beam [12,13]. The method was then adapted for measurements at zero degrees to observe unbound nuclei beyond the dripline [14–16].

Up to now, measurements at zero degrees using this method have been limited to light nuclei ($Z \leqslant 4$) produced with light primary beams ($Z \sim 8$). In the present work, we explore the feasibility of using SNDS as a technique to study heavier isotopes starting with a primary beam of ^{48}Ca.

2. Experimental setup

The experiment was performed at the National Superconducting Laboratory (NSCL) at Michigan State University. The primary beam of ^{48}Ca was accelerated to 90 MeV/u using the coupled K-500 and K-1200 cyclotrons. In order to allow reaction products to be bent by the sweeper magnet (see below), the beam was degraded to 60 MeV/u in the A1900 fragment separator [17]. It was then delivered to a 94 mg/cm^2 beryllium reaction target. Charged fragments produced in the reaction were first sent through a focusing quadrupole triplet and then deflected through a large gap sweeper magnet [18]. Neutrons produced in the reaction were detected by the Modular Neutron Array (MoNA) [19,20] located at zero degrees. A schematic of the experimental setup can be seen in Fig. 1.

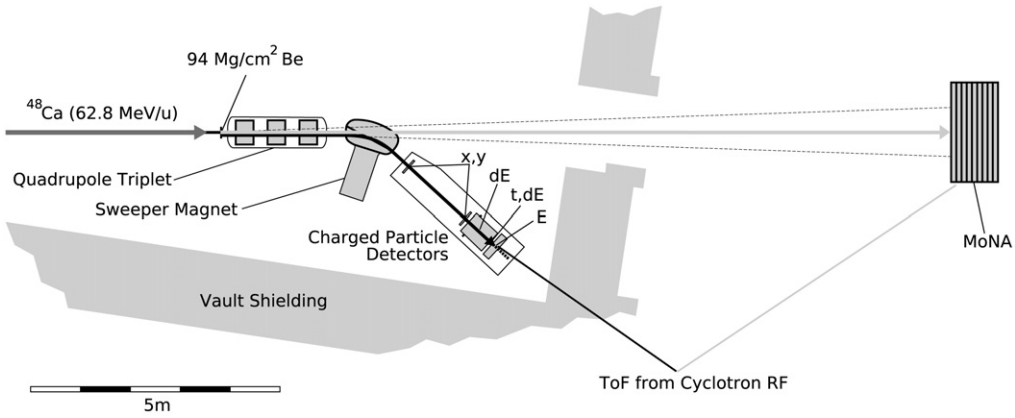

Fig. 1. Experimental setup.

The dipole sweeper magnet has a bending angle of 43° and a vertical gap of 14 cm. A large vacuum chamber is located behind the magnet containing detectors used to measure position, timing, and energy information of the charged fragments. During the experiment, the sweeper was set to a magnetic rigidity of 2.99 Tm, and a tungsten beam blocker was placed on the low rigidity side of the magnet in order to block unreacted beam particles from the detectors. The focal plane detectors used during the run were a pair of 30 mm × 30 mm cathode readout drift chambers (CRDCs) located 182 cm apart to measure position and angle; a 65 cm long ion chamber to measure energy loss; and a thin 4.5 mm plastic scintillator to measure time of flight (ToF). The start signal for all events was provided by the cyclotron radio frequency (RF) signal.

MoNA is an array of 144 plastic scintillator modules, each 10 cm high × 200 cm wide × 10 cm deep. The scintillation light is detected on both ends by photomultiplier tubes (PMTs). ToF is determined by the mean of the timing signals of the two PMTs, while horizontal position is determined by the time difference between the two PMT signals. Vertical and lateral positions are determined based on the module in which the neutron interacts. In the present experiment, MoNA was arranged in a configuration 16 modules high by 9 modules deep, and the front face was placed at a distance of 15.38 m from the reaction target. Neutrons were shadowed horizontally by the opening bore of the triplet and vertically by the gap of the sweeper magnet, resulting in an angular acceptance of ±1.5° in the vertical direction and $^{+2.5}_{-2.0}$ degrees in the horizontal direction.

3. Data analysis

The charged fragments are separated and identified using energy loss and ToF measurements. The element (Z) identification is based primarily on the energy loss in the ion chamber, while the mass number (A) is determined using the ToF. Due to the large momentum acceptance of the sweeper magnet, the ToF must be corrected based on dispersive position and angle at the focal plane. This correction is achieved by applying position and angle correction factors:

$$t_{\text{corr}} = t + c_x \cdot x + c_\theta \cdot \theta, \tag{1}$$

where c_x and c_θ are empirically determined constants. Due to nonuniformities of the magnetic field, the correction factors depend on the particle's location in angle-position phase space. To

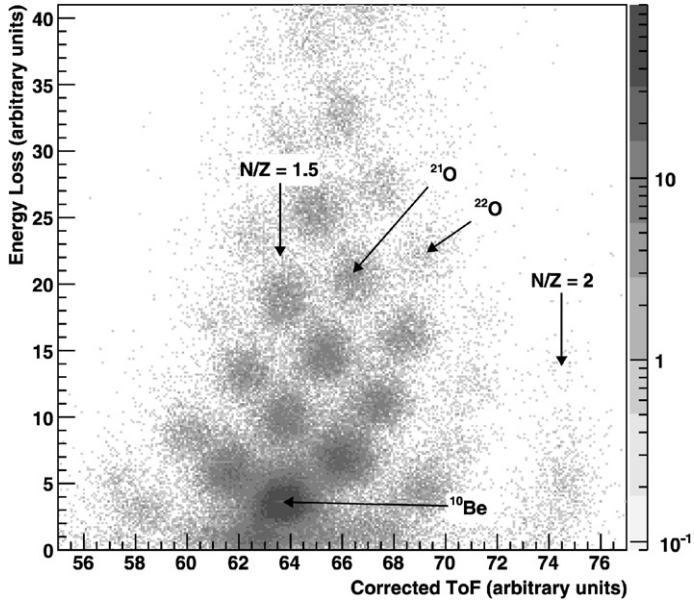

Fig. 2. Sample particle identification plot. The vertical $N/Z = 2$ and $N/Z = 1.5$ bands, along with selected isotopes, are indicated.

account for this effect, the phase space is divided into a 5×6 grid, and separate correction factors are determined for each grid region. Fig. 2 shows a sample particle ID plot for one grid region.

Neutrons are identified by ToF as shown in Fig. 3. The peak around 150 ns is due to fast neutrons produced in the reaction target with a velocity close to the beam velocity. Prompt γ-rays are cleanly separated. Background events are subtracted as described in the next section.

In the earlier SNDS experiments [12–16], the excited states were identified by their relative velocity spectra. The angular acceptance of these experiments was small, so that the approximation $E_{\text{decay}} \simeq \mu v_{\text{rel}}/2$ could be applied, where μ is the reduced mass, and the relative velocity, $v_{\text{rel}} = v_{\text{n}} - v_{\text{f}}$, is the difference between the neutron (v_{n}) and fragment (v_{f}) velocities.

The angular acceptance in the present experiment was also limited, primarily due to the focusing quadrupole. However, the neutron and fragment emission angles can be extracted to determine the E_{decay} directly via the invariant mass method:

$$E_{\text{decay}} = \sqrt{m_{\text{f}}^2 + m_{\text{n}}^2 + 2(E_{\text{f}} \cdot E_{\text{n}} - p_{\text{f}} \cdot p_{\text{n}} \cdot \cos\theta_{\text{open}})} - m_{\text{f}} - m_{\text{n}}. \tag{2}$$

The equation contains the masses, energies and momenta of the neutrons (m_{n}, E_{n}, p_{n}) and the fragments (m_{f}, E_{f}, p_{f}) as well as the opening angle, θ_{open}, between the two particles.

The neutron angle is calculated from the measured interaction point in MoNA, and the energy and momentum are calculated using ToF and flight distance. For the charged fragment, energy is calculated using ToF and path length, while the angle is reconstructed based on position and angle measurements made with the CRDC detectors. This reconstruction utilizes a partial-inverse matrix [21] produced with COSY INFINITY [22].

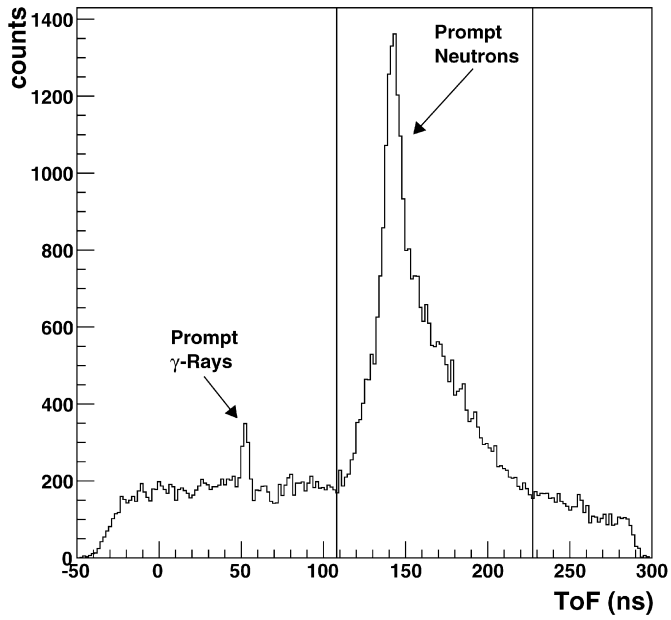

Fig. 3. MoNA ToF spectrum, gated on ^{10}Be, showing clear separation between prompt neutrons and prompt γ-rays.

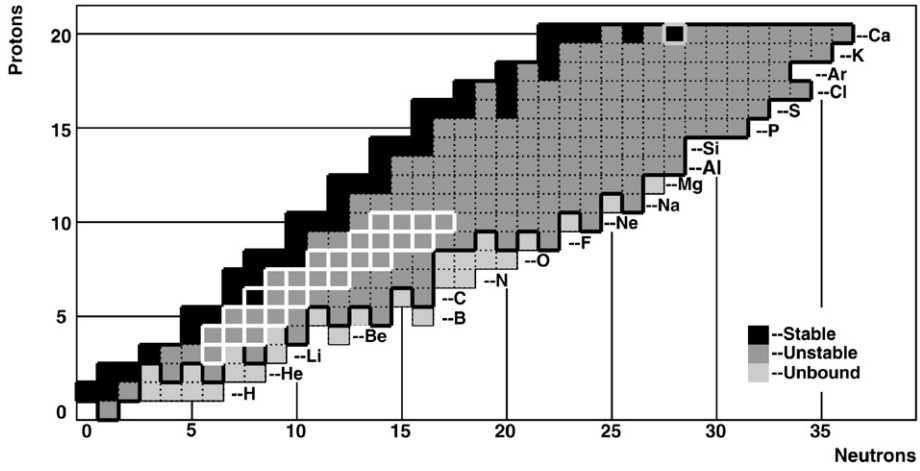

Fig. 4. Chart of the nuclides. Isotopes outlined in white were observed in sufficient quantities to be studied.

4. Results and discussion

The fragments which could be identified and separated and which were produced in sufficient quantities to be studied are indicated on a chart of nuclides in Fig. 4. The range of fragments is determined by the magnetic rigidity ($B\rho$) and the momentum acceptance of the sweeper magnet. For $Z > 10$ the ToF resolution is not sufficient to separate neighboring isotopes.

Fig. 5 shows relative velocity spectra for the three most prevalent fragments of each element

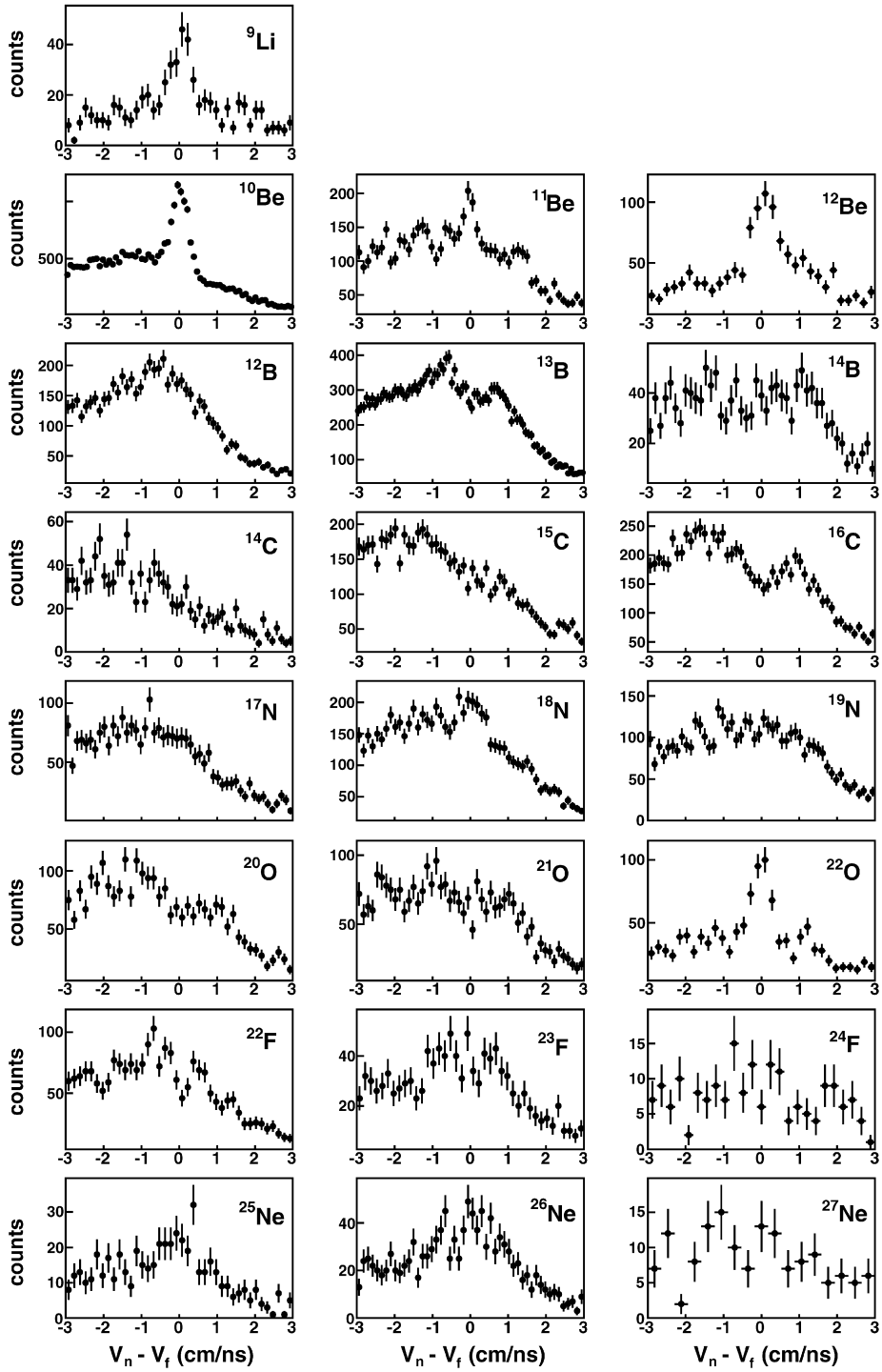

Fig. 5. Velocity difference (neutron minus fragment) for the most prevalent isotopes.

from lithium through neon. Most fragments, including those not displayed in the figure, have a rather broad shape indicative of a non-resonant distribution. Only the spectra of ^{9}Li, ^{10}Be, ^{12}Be, and ^{22}O show a peak near zero relative velocity. These peaks suggest the presence of a neutron-unbound state with a small decay energy. The enhancement near zero relative velocity in ^{11}Be is attributed to contamination from ^{10}Be.

The observations from the relative velocity spectra are confirmed by the decay energy spectra displayed in Fig. 6. While ^{9}Li, ^{10}Be, ^{12}Be, and ^{22}O all display a narrow peak at low decay energies, the other fragments have a broad featureless distribution.

That only low decay energy states are observed is not surprising and is due to the limited angular acceptance of the experimental setup. Fig. 7 shows the efficiency of the setup as a function of decay energy for a Monte Carlo simulation [23] of a flat decay energy distribution from 0 to 1 MeV. The efficiency peaks at zero decay energy and then falls off rapidly as the energy increases. This demonstrates a major limitation of the method. The small angular acceptance is determined by the 4 inch bore diameter of the focusing quadrupole magnet and the 14 cm vertical gap of the sweeper magnet. These components are essential for the identification of the isotopes. In order to increase the acceptance, significant modifications such as placing the focusing quadrupole behind the sweeper magnet would need to be made to the experimental setup.

In the following, the spectra of the four isotopes showing evidence for the presence of a low energy neutron decay state are analyzed in more detail. The intent of this analysis is not to make independent measurements of the decay properties of these nuclei, but rather to confirm that the present data are consistent with previous measurements.

Monte Carlo simulations, including the experimental resolutions and acceptances, were performed with the decay parameters for each individual isotope taken from the literature. The results of these simulations and experimental data for each isotope are shown in Fig. 8. In the figure, background contributions calculated by event mixing were subtracted from the data. The fragments of ^{9}Li, ^{10}Be, ^{12}Be, and ^{22}O originate from states in ^{10}Li, ^{11}Be, ^{13}Be, and ^{23}O, respectively. The figure includes the level schemes and proposed states for each observed decay.

4.1. ^{10}Li

The ground state of ^{10}Li lies slightly above the one-neutron emission threshold [14,15,24] and is known to be an s-wave state [25]. Experiments measuring ground state properties of ^{10}Li are analyzed in terms of the scattering length a_s, and the most recent measurements [24] extract $a_s = -30^{+12}_{-31}$ fm. In the present work, the decay energy of ^{10}Li into $^{9}\mathrm{Li} + n$ is simulated assuming an s-wave interaction using the model described in Ref. [15]. The best fit to the data that is consistent with Ref. [24] is with $a_s = -50$ fm; it is shown in the top left panel of Fig. 8.

4.2. ^{11}Be

The ground state of ^{11}Be is bound against particle decay, with a one-neutron separation energy of 504 keV [26]. The lowest lying unbound excited state is located at 1778 keV [27]. A previously observed low energy neutron decay originating from ^{11}Be has been attributed to a decay to the first excited 2^+ state at 3368 keV in ^{10}Be [11,13,29]. Deák et al. [13] quote a decay energy of 19(15) keV and assign this decay to the 3887(15) keV state in ^{11}Be [27]. Peters et al. [29] state a decay energy of 84(15) originating from the 3956(15) keV $3/2^-$ state in ^{11}Be [27]. Pain

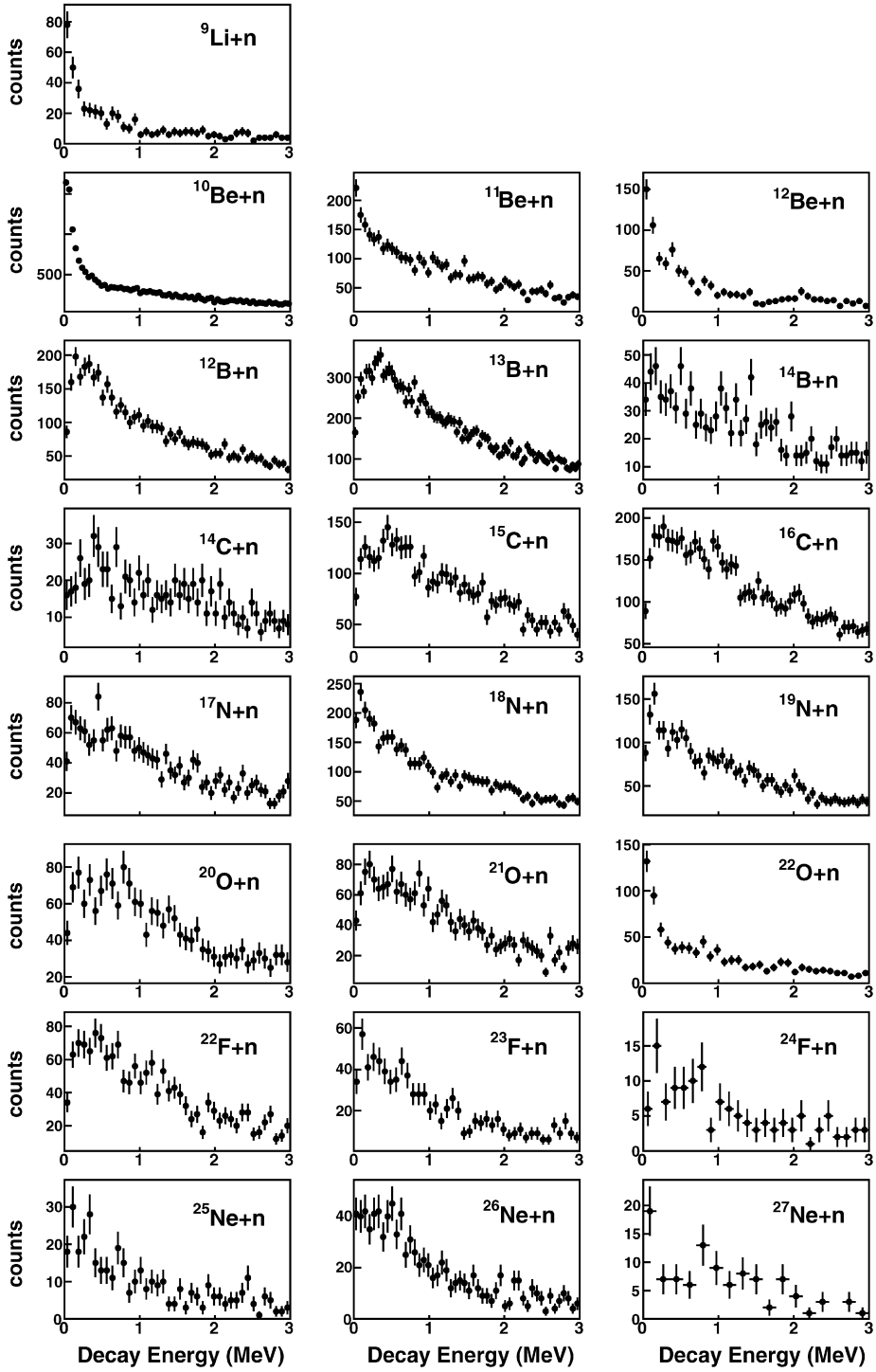

Fig. 6. Decay energy spectra for the most prevalent isotopes.

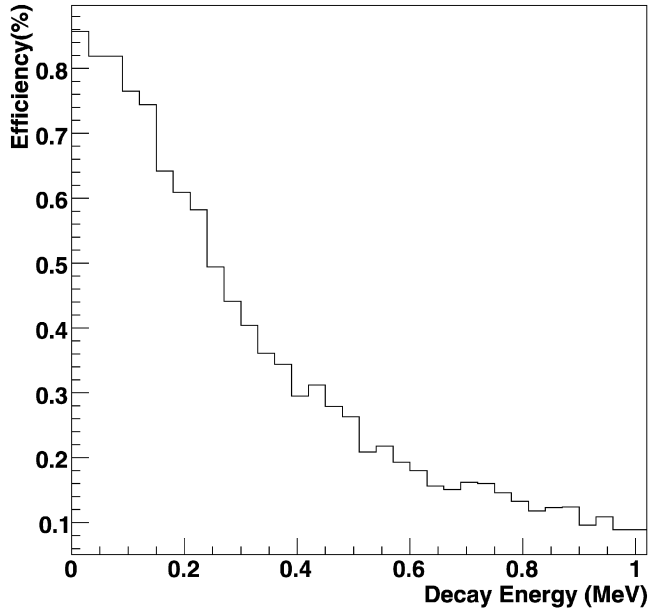

Fig. 7. Efficiency of the experimental setup as a function of decay energy.

et al. [11] do not attempt to assign the decay to a specific state in ^{11}Be and remark that the decay originates from excited ^{11}Be at approximately 4.0 MeV.

One-neutron knockout reactions selectively populate only specific states; hence it is possible that the low energy state at 19 keV of Ref. [13] was not observed by Refs. [11,29]. On the other hand, the relative velocity spectrum of Ref. [13] was probably not sensitive enough to resolve a possible contribution of the state at 84 keV observed in Refs. [11,29]. Thus, the present decay of ^{11}Be to ^{10}Be + n is simulated with two Breit–Wigner resonances as described in [6]. The energies and widths of the two decays are $E_{\text{decay}} = 19$ keV; $\Gamma_{\text{decay}} = 10$ keV and $E_{\text{decay}} = 84$ keV; $\Gamma_{\text{decay}} = 10$ keV, based on the level assignments of Deák et al. [13] and Peters et al. [29], respectively. The widths for both decays are set to the upper limit of 10 keV taken from Ref. [26]. Relative contributions from each of the two states are treated as free parameters, and the best fit to the data is achieved with a 53% contribution from the 19 keV decay and a 47% contribution from the 84 keV decay. The fit is shown in the upper right corner of Fig. 8, along with the contributions from the 19 keV resonance (dashed line) and the 84 keV resonance (dotted line).

It should be mentioned that the data could also be described by a single resonance, with a resonance energy of $E_{\text{decay}} = 30$ keV and a resonance width of $\Gamma_{\text{decay}} = 65$ keV.

4.3. ^{13}*Be*

An SNDS experiment from a primary ^{18}O beam observed a low-lying s-wave resonance with a scattering length of $a_s < -10$ fm as the ground-state of ^{13}Be [16]. However, the authors were not able to rule out the possibility that the low lying resonance they observed was due to a p or d state at $E_{\text{decay}} = 50(10)$ keV with a width of $\Gamma_{\text{decay}} \leqslant 10$ keV. Subsequent experiments using a single proton-knockout reaction from ^{14}B [30] or single neutron-knockout from ^{14}Be [24] failed

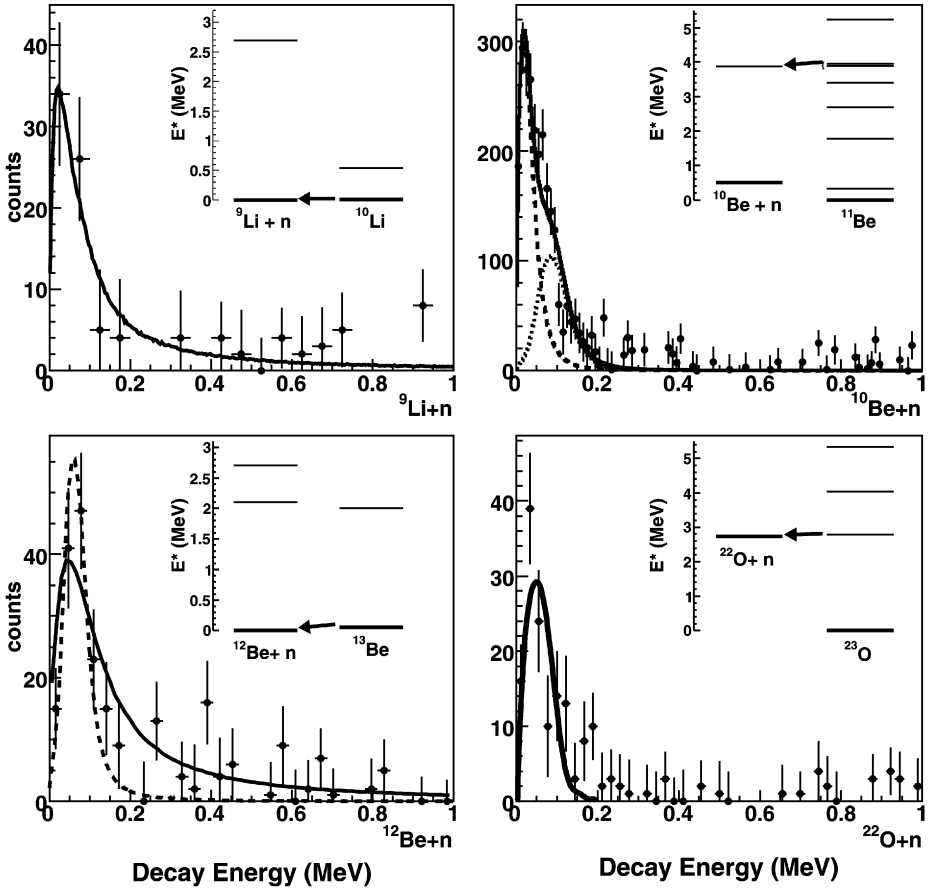

Fig. 8. Background subtracted decay energy spectra (filled circles), with results from Monte Carlo simulations (lines); for ^{12}Be, both s-wave (solid line) and Breit–Wigner (dashed line) fits are shown. The fit for ^{10}Be includes contributions from both the 19 keV (dashed line) and 84 keV (dotted line) resonances. Simple level schemes showing the measured decays are also included. Levels for the two highest excited states in ^{23}O come from Ref. [28], and the lowest lying state in ^{23}O is from Ref. [6]; all other levels are taken from Ref. [26].

to observe a low lying resonance in ^{13}Be. Instead a strong resonance at approximately 700 keV was reported.

The present decay spectrum for $^{12}\mathrm{Be} + n$ indicates a low-energy decay similar to Ref. [16]. The lower left panel of Fig. 8 shows the results of fits using an s-wave (solid line) and a Breit–Wigner resonance (dashed line). The parameters used for the fits are $a_s = -20$ fm (s-wave) and $E_{\mathrm{decay}} = 60$ keV, $\Gamma_{\mathrm{decay}} = 10$ keV (Breit–Wigner), based on the results presented in Ref. [16].

4.4. ^{23}O

The unbound first excited state of ^{23}O has recently been measured by Schiller et al. [6] in the two-proton knockout reaction from ^{26}Ne. The observed decay energy of $E_{\mathrm{decay}} = 45(2)$ keV places the resonance at an excitation energy of 2.8(1) MeV in ^{23}O. The present results, shown in the lower right panel of Fig. 8, also indicate a resonance at a very low decay energy. The fit shown

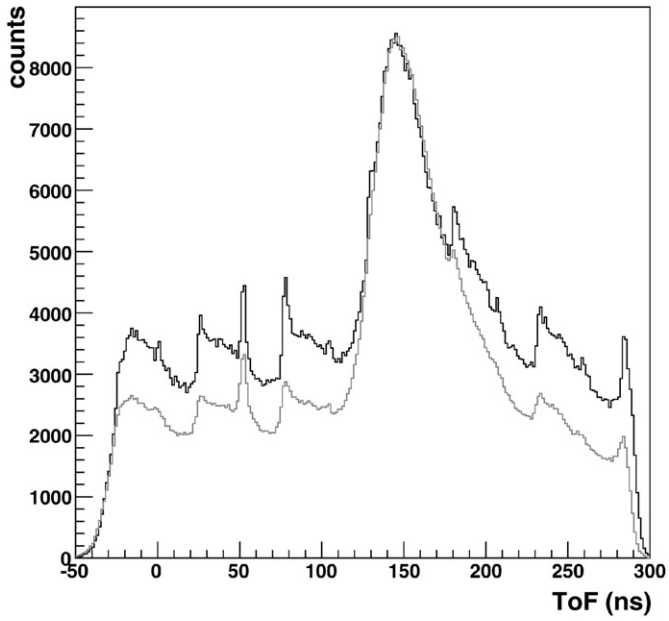

Fig. 9. Neutron ToF for production (grey) and high-rate (black) runs. The data are normalized to each other at the maximum of the fast neutron peak.

in the figure corresponds to a Breit–Wigner resonance with $E_{\text{decay}} = 45$ keV and $\Gamma_{\text{decay}} = 5$ keV, consistent with the resonance parameters in Ref. [6].

5. Future prospectives

The present experiment reaches nuclei beyond the dripline only for the lightest elements (^{10}Li and ^{13}Be). Fig. 2 shows that for heavier elements the populated nuclei are significantly removed from the dripline. In order to observe decays of more neutron-rich nuclei, the magnetic rigidity of the sweeper magnet was increased to $B\rho = 3.14$ Tm. This corresponds to a shift of about one isotope for neon. The cross section to populate these nuclei decreases, so the primary beam intensity had to be increased to compensate, and this higher beam rate increased the random background rate of neutron events. Fig. 9 shows the neutron ToF for one of the production runs for the data shown in Section 4 (grey line) and a high-rate run (black line). The periodic features of the random background correspond to the cyclotron frequency. The increasing random-to-real ratio makes it more difficult to extract the signal from unbound resonances. Already the small shift of one isotope towards the dripline increases the background rate by about 40%. Thus it was impossible to reach the dripline for the heavier elements using the present experimental configuration.

In the future, SNDS could be extended to higher decay energies as well as heavier masses. The angular acceptance could be increased by substituting the quadrupole with the S800 spectrograph [31]. The target could be placed immediately in front of the sweeper magnet which would eliminate the shadowing of MoNA due to the small bore of the quadrupole. The increased flight path and higher resolution of the S800 will also enable isotopic separation up to significantly heavier elements.

However, it does not appear to be possible to populate and measure the decay of neutron unbound states closer to the neutron dripline with SNDS in the near future. The small cross section for the production of the dripline nuclei with stable beams requires large beam intensities which in turn generate a large number of neutrons from unrelated reactions. In the longer term, SNDS could be used at the next generation radioactive beam facilities [32]. The unbound states would then be populated by intense secondary beams closer to the dripline nuclei of interest.

6. Summary and conclusion

The method of sequential neutron decay spectroscopy (SNDS) has been applied for the first time using medium mass projectiles (^{48}Ca). The method succeeded in populating and identifying unbound ground states of ^{10}Li and ^{13}Be as well as unbound excited states in ^{11}Be and ^{23}O. The extracted resonance parameters were consistent with values reported in the literature. The common feature of these states is their small decay energy ($<$100 keV). The small angular acceptance of the experimental setup for neutrons limited the observation to unbound states with small decay energies. Isotopic separation could be achieved up to neon and was limited by the ToF resolution for the charged particles.

The future study of neutron unbound states with higher decay energies will require significant modifications of the experimental setup. The measurement of masses of nuclei beyond the dripline using SNDS will have to wait for the next generation radioactive beam facilities.

Acknowledgements

The authors are grateful to the staff of the NSCL for providing a high-quality beam throughout the experiment. This work was supported by the National Science Foundation under grants Nos. PHY-01-10253, PHY-03-54920, PHY-04-56463, PHY-05-55366, PHY-05-55488, PHY-05-55445 and PHY-06-06007, with funding for the two REU students D.Al. and A.M.H. provided by grant PHY-02-43709.

References

[1] R. Kalpakchieva, et al., Eur. Phys. J. A 7 (2000) 451.
[2] G. Bohlen, et al., Eur. Phys. J. A 31 (2007) 279.
[3] A.A. Korsheninnikov, et al., Phys. Rev. Lett. 82 (1999) 3581.
[4] A.H. Wuosmaa, et al., Phys. Rev. C 72 (2005) 061301(R).
[5] F. Skaza, et al., Phys. Rev. C 73 (2006) 044301.
[6] A. Schiller, et al., Phys. Rev. Lett. 99 (2007) 112501.
[7] C.S. Sumithrarachchi, et al., Phys. Rev. C 75 (2007) 024305.
[8] K.W. Scheller, et al., Phys. Rev. C 49 (1994) 46.
[9] Z. Radivojevic, et al., Nucl. Instrum. Methods Phys. Res. A 481 (2002) 464.
[10] M. Zinser, et al., Nucl. Phys. A 619 (1997) 151.
[11] S.D. Pain, et al., Phys. Rev. Lett. 85 (2000) 266.
[12] F. Deák, et al., Phys. Rev. C 52 (1995) 219.
[13] F. Deák, et al., Nucl. Instrum. Methods Phys. Res. A 258 (1987) 67.
[14] R.A. Kryger, et al., Phys. Rev. C 47 (1993) R2439.
[15] M. Thoennessen, et al., Phys. Rev. C 59 (1999) 111.
[16] M. Thoennessen, S. Yokoyama, P.G. Hansen, Phys. Rev. C 63 (2000) 014308.
[17] D.J. Morrissey, et al., Nucl. Instrum. Methods Phys. Res. B 204 (2003) 90.
[18] M.D. Bird, et al., IEEE Trans. Appl. Superconduct. 15 (2005) 1252.
[19] B. Luther, et al., Nucl. Instrum. Methods Phys. Res. A 505 (2003) 33.

[20] T. Baumann, et al., Nucl. Instrum. Methods Phys. Res. A 543 (2005) 517.
[21] N. Frank, et al., Nucl. Instrum. Methods Phys. Res. A 580 (2007) 1478.
[22] K. Makino, M. Berz, Nucl. Instrum. Methods Phys. Res. A 558 (2005) 346.
[23] H. Scheit, Simple Track for MoNA, 2006, NSCL.
[24] H. Simon, et al., Nucl. Phys. A 791 (2007) 267.
[25] M. Chartier, et al., Phys. Lett. B 510 (2001) 24.
[26] G. Audi, O. Bersillon, J. Blachot, A.H. Wapstra, Nucl. Phys. A 624 (1997) 1.
[27] F. Ajzenberg-Selove, J.H. Kelley, Nucl. Phys. A 506 (1990) 1.
[28] Z. Elekes, et al., Phys. Rev. Lett. 98 (2007) 102502.
[29] W.A. Peters, PhD thesis, Michigan State University, 2007 (unpublished);
W.A. Peters, et al., in preparation.
[30] J.L. Lecouey, Few Body Syst. 34 (2004) 21.
[31] D. Bazin, et al., Nucl. Instrum. Methods B 204 (2003) 629.
[32] D.F. Geesaman, C.K. Gelbke, R.V.F. Janssens, B.M. Sherrill, Annu. Rev. Nucl. Part. Sci. 56 (2006) 53.